

Electronic Structure and Anisotropy of X-Ray Emission Spectra of $\text{NaV}_6\text{O}_{15}$ Monocrystal

V. M. CHERKASHENKO,* S. P. FREIDMAN,^{†1} V. A. GUBANOV,[†]
E. Z. KURMAEV,* V. L. VOLKOV,[†] AND A. A. FOTIEV[†]

* *Institute of Metal Physics and* [†] *Institute of Chemistry, Ural Science Center, Academy of Sciences of the USSR, Sverdlovsk, USSR*

Received December 7, 1978; in final form July 26, 1979

The electron structure of $\text{NaV}_6\text{O}_{15}$ bronze was investigated by measuring the orientation dependence of the X-ray emission $VK_{\beta''\beta_5}$ and VK_{β_1} spectra in $\text{NaV}_6\text{O}_{15}$ monocrystal and by performing quantum-chemical cluster calculations. On the base of results obtained, it is concluded that there is preferred delocalization of valence electrons in the V_1 and V_2 atom chains along the b axis.

Introduction

During the past several years many investigators have paid serious attention to vanadium compounds with mixed valency, in particular, to oxide vanadium bronzes of the $M_xV_2O_5$ type. An increased interest in such compounds is due to properties which make them promising materials for thermoresistors, electrode materials, and catalysts. There are numerous investigations of the physical properties of these bronzes, but among the specialists, unanimous agreement about their origin has not been achieved.

In (1) we studied X-ray emission $K_{\beta''\beta_5}$ ($1s-4p$ transition) and L_α ($2p-3d$, $4s$ transition) vanadium spectra and K_α oxygen spectra in polycrystalline specimens of oxide vanadium bronzes. In the present paper we continue study of the electronic structure of these compounds by investigation of the orientation dependence of $K_{\beta''\beta_5}$ and K_{β_1} vanadium spectra and by performing quantum-chemical calculations.

The crystal structure of vanadium bronze $\text{NaV}_6\text{O}_{15}$ has been studied in (2). This compound has a highly anisotropic structure, in which the vanadium atoms can be situated in three nonequivalent positions (Fig. 1). Distorted octahedra are the nearest environment for all possible positions of the V atoms. In each octahedron the V-O bond lengths in the ac plane vary within wide limits (from 1.56 to 2.68 Å) whereas in the b direction V-O distances are nearly equal (1.90 Å). The oxygen polyhedra, joined by corners and edges, form tunnels along the b axis in which Na atoms are arranged.

Investigations of the electrical conductivity show the presence of quasi-one-dimensional properties for $\text{NaV}_6\text{O}_{15}$ monocrystal, i.e., conductivity of the semiconducting type along the b axis exceeding by two orders of magnitude that in the plane normal to the b axis (3, 4). Moreover, MV_6O_{15} monocrystal, annealed in vacuum, undergoes a one-dimensional phase transition of the semiconductor-metal type along the b axis (4, 5).

¹ To whom correspondence should be addressed.

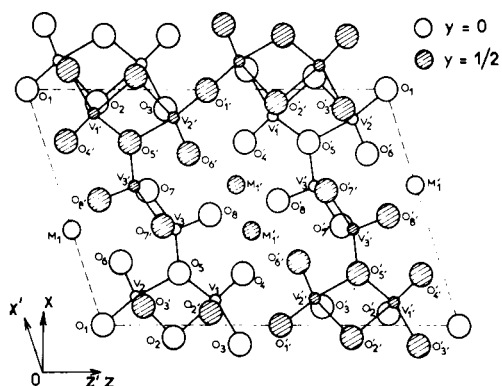


FIG. 1. Crystal structure of oxygen vanadium bronze $\text{NaV}_6\text{O}_{15}$.

As follows from the chemical formula of the $\text{NaV}_6\text{O}_{15}$ compound and its crystal structure, one Na atom accounts for six V atoms, occupying three nonequivalent positions in the crystal. In (1, 6, 7) it has been established that M atoms give their electrons to the vanadium–oxygen sublattice and do not participate in formation of an electron energy spectrum for the compound. However, rather contradictory opinions exist about the place of such electron localization in the vanadium–oxygen sublattice. On the one hand, experimental evidence exists for localization of Na electrons on V ions with the formation of V^{4+} centers, and, on the other hand, some arguments speak for preferable delocalization of these electrons in the vanadium–oxygen sublattice (1, 9, 10). The question of the localization of the Na valence electron in the compound under consideration will be discussed in the present paper using data from an experimental investigation of the orientation dependence for vanadium X-ray emission spectra and theoretical quantum–chemical calculations of clusters in $\text{NaV}_6\text{O}_{15}$.

Experimental

Study of the anisotropy of X-ray emission spectra from nonocrystals allows one to

obtain additional information about the electron structure of substances as compared with information obtained from investigation of polycrystalline samples (11–13). In the case of K spectra, transitions polarized in directions parallel to the x , y , or z axis are connected accordingly with np_x , np_y , or np_z states. Because of the character of electromagnetic waves, radiation polarized, for instance, parallel to the y axis cannot spread in this direction. Furthermore, if the angle of the incident wave on the crystal analyzer is equal to 45° , it is possible to turn off the radiation with the vector of polarization ϵ coinciding with the direction of the reflected beam. In our case, the angle of the incident wave was about 43° and, therefore, the reflected radiation had almost complete polarization.

X-Ray VK emission spectra were obtained under the same conditions as the spectra of polycrystalline $\text{NaV}_6\text{O}_{15}$ which was investigated by us previously in Ref. (1). The investigation of the VK emission spectra was performed for two different orientations of a $\text{NaV}_6\text{O}_{15}$ monocrystal. In the first case, the \mathbf{b} axis of the monocrystal was situated perpendicular to the plane of the Rowland circle; hence, the conditions for reflection of radiation, polarized along the one-dimensional b axis, were fulfilled. In the second case, the \mathbf{b} axis was directed toward the crystal analyzer and only the components of radiation, polarized in the plane normal to the \mathbf{b} axis ($\epsilon \perp \mathbf{b}$), were registered. For such polarization $4p_x$ and $4p_z$ states give equal contributions to the intensity (in the xz plane, the monocrystal was not oriented). Though the emitter had limited dimensions and the monocrystals were visually oriented with reference to the crystal analyzer, in the first approximation one can consider that the spectrum with $\epsilon \parallel \mathbf{b}$ reflected the distribution of $4p_y$ states only and in the spectrum with $\epsilon \perp \mathbf{b}$ only the $4p_x$ and $4p_z$ components took part equally. Thus, for intensities of these spectra one can write the relations:

$$I_{\parallel} = I_{4p_y}; \quad I_{\perp} = \frac{1}{2}(I_{4p_x} + I_{4p_z}). \quad (1)$$

For the intensity of the $VK_{\beta''\beta_5}$ spectrum of a polycrystalline sample, the analogous relation is as follows:

$$I_{\text{pol.}} = I_{4p_y} + I_{4p_x} + I_{4p_z} = I_{\parallel} + 2I_{\perp} \quad (2)$$

Therefore, the VK spectrum for polycrystalline $\text{NaV}_6\text{O}_{15}$ can be obtained by summation of I_{\parallel} and I_{\perp} spectral intensities. The results (see Fig. 2) show that when the maximum intensities of the VK_{β_5} bands are equal, the best coincidence between additive and experimental (I) spectra is observed. Taking this circumstance into account, it follows from Eq. (2) that I_{\parallel} and I_{\perp} intensities of the VK_{β_5} band are related as 2:1, but a true relation of spectral subbands with $\epsilon \parallel \mathbf{b}$ and $\epsilon \perp \mathbf{b}$ is as presented in Fig. 3. It is seen that the anisotropy of the $VK_{\beta''\beta_5}$ spectra is manifested on the whole as a redistribution of the $K_{\beta''}$ and K_{β_5} band intensities. On going from the $\epsilon \parallel \mathbf{b}$ spectrum to the $\epsilon \perp \mathbf{b}$ spectrum, the intensity of the $K_{\beta''}$ band does not change, but the intensity of the K_{β_5} band decreases by a factor of 2. This results in an increase of the relative intensity $I_{K_{\beta''}}/I_{K_{\beta_5}}$ from 47 to 95%, whereas in the spectrum of a polycrystal this value amounts to 72% (I). The width of the VK_{β_5} band, measured at the half-height of the intensity maximum, decreases in this case from 5.2 to 4.6 eV at the expense of the long-wave part (Fig. 2). Furthermore, the anisotropy reveals itself also in the $K_{\beta''}$ band, possessing three elements of structure. In the $\epsilon \parallel \mathbf{b}$ spectrum, the high-energy part of the

band ($\mathbf{1}$ in Fig. 3) is absent, but in the $\epsilon \perp \mathbf{b}$ spectrum all three structural elements are resolved. So, the structure of the $K_{\beta''}$ band (I) (Fig. 2) discovered in the $VK_{\beta''\beta_5}$ spectra of MV_6O_{15} polycrystals is due to the high-energy hump ($\mathbf{1}$) in the $\epsilon \perp \mathbf{b}$ spectrum and is connected consequently with $4p_x$ and $4p_z$ states. It should be recalled that the appearance of this structure element in the $\epsilon \parallel \mathbf{b}$ spectrum is connected with noncomplete polarization of the X-ray radiation in our experiments.

The anisotropy of the characteristic X-ray radiation is manifested also in the VK_{β_1} spectrum (Fig. 4). The intensity maximum of the K_{β_1} spectrum polarization shows itself in a way analogous to that of the K_{β_5} band: one can observe a two fold increase of I_{\parallel} in comparison with I_{\perp} , measuring relative to the $K_{\beta''}$ band. The width of the K_{β_1} line, measured at half-height of the intensity maximum, changes in an opposite direction compared with the K_{β_5} band, i.e., it increases from $\epsilon \parallel \mathbf{b}$ to $\epsilon \perp \mathbf{b}$ by ~ 0.6 eV. Apparently, it is due to K_{β_5} band anisotropy dependence on both splitting of $4p$ states in the crystal field and effects of overlapping with $\text{O}2p$ states. However, the anisotropy of the K_{β_1} line is due only to splitting of the $3p$ states of V in a crystal field of noncubic symmetry. The increase of width and the decrease of the K_{β_1} spectrum intensity for $\epsilon \perp \mathbf{b}$ is caused, perhaps, by splitting of $3p_x$ and $3p_z$ states, one of which (different for each of the V_1 , V_2 , and V_3 octahedra) coincides in energy with the

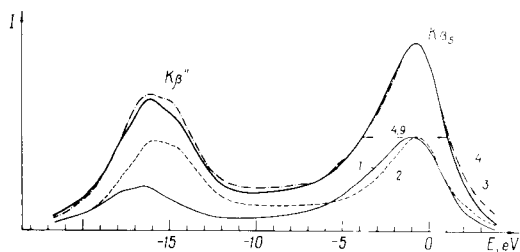


FIG. 2. Comparison of additive (3) and experimental (4) $K_{\beta''\beta_5}$ spectra in vanadium bronze $\text{NaV}_6\text{O}_{15}$: (1) $\epsilon \parallel \mathbf{b}$; (2) $\epsilon \perp \mathbf{b}$.

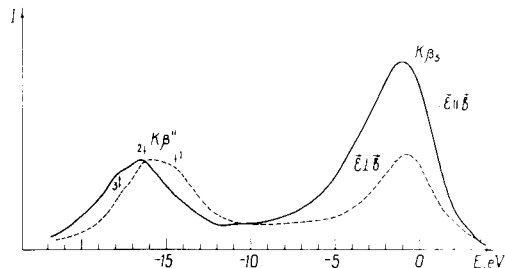


FIG. 3. True intensity relations of polarized $VK_{\beta''\beta_5}$ spectra for $\text{NaV}_6\text{O}_{15}$.

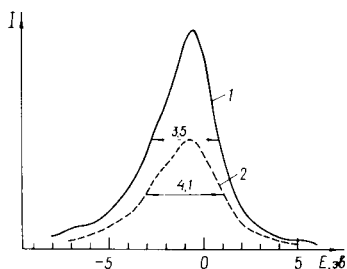


FIG. 4. Anisotropy of the VK_{β_1} line for $\text{NaV}_6\text{O}_{15}$ monocystals: (1) $\epsilon \parallel \mathbf{b}$; (2) $\epsilon \perp \mathbf{b}$.

$3p_y$ state in the $\epsilon \parallel \mathbf{b}$ spectrum. It is not possible to identify the $3p_x$ and $3p_y$ states more precisely, as three nonequivalent octahedra are oriented differently relative to the crystal axes (Fig. 1).

Calculation of the Electron Structure of Clusters

For the description of the electron structure of the oxygen–vanadium sublattice in the bronze under consideration, quantum-chemical calculations of clusters, including the V atom and its nearest environment, have been performed. The coordinate system (x, y, z) used in the calculations is shown in Fig. 1.

The main part of the calculations was carried out by the semiempirical Mulliken–Wolfsberg–Helmholz (MWH) method with self-consistency on charges and configurations (14–16). The same method of parameterization and the same wavefunctions were used in (17, 18). Moreover, for comparison, nonself-consistent calculations of clusters were carried out by the discrete variational method (DVM) (19, 20).

In view of the fact that the localization site of the Na valence electron in the oxygen–vanadium sublattice is not known, calculations of $(\text{VO}_6)^{7-}$ clusters (48 valence electrons) for the V_1 , V_2 , and V_3 sites and $(\text{VO}_6)^{8-}$ clusters (49 valence electrons) for the same sites were performed. For convenience in further discussion we refer to

these clusters as $V_n m$, where n is the type of site and m is the number of cluster valence electrons. The $(\text{VO}_6)^{8-}$ cluster (78 core and valence electrons + Na valence electron) was calculated by $X\alpha$ DVM in the spin-polarized variant. The calculations of $(\text{VO}_6)^{7-}$ (78 core and valence electrons) for the V_2 - and V_3 -type sites were carried out by the spin-restricted $X\alpha$ DVM version. The numerical basis set of atomic wavefunctions, obtained in the calculation of V and O atoms by Herman–Skillman programs (21), was used in the calculations; 900 $\{\mathbf{r}_k\}$ points were used for the calculation of the matrix elements (19, 20).

The MO energy diagrams, obtained in the MWH and DVM calculations, are shown in Fig. 5. The character of the energy spectrum in all the calculations performed proves to be the same. There exist two groups of energy levels in the spectrum. The main contributions in the molecular orbitals (MO) of the first group, consisting of six levels, give 2s ligand states. These orbitals also have about 5% $V3d$ and $V4s$ admixture. The second group of 18 energy levels is situated higher on the energy scale. The corresponding MO's have 2p ligand character with admixture (about 25%) of $V3d$ AO and a smaller admixture of $V4s$, $V4p$, and $O2s$ AO. The less compact group of five MO is placed at about 1.7–3.5 eV. The contribution of $V3d$ AO's in these MO's reaches up to 50–60%. Other contributions belong to $O2p$ AO's and, to a lesser extent, $O2s$. We call the cited groups of levels $O2s$, $O2p$, and $V3d$ bands, respectively.

It should be noted that MO diagrams, obtained in the DVM calculations, have a systematic shift in energy of 6–7 eV in comparison with the diagrams obtained from the MWH calculations. It could be the result of non-self-consistency of the DVM calculations.

The data on the electron structure of clusters are listed in Tables I and II. As is seen, the populations of the $V3d$, $V4s$, and $V4p$

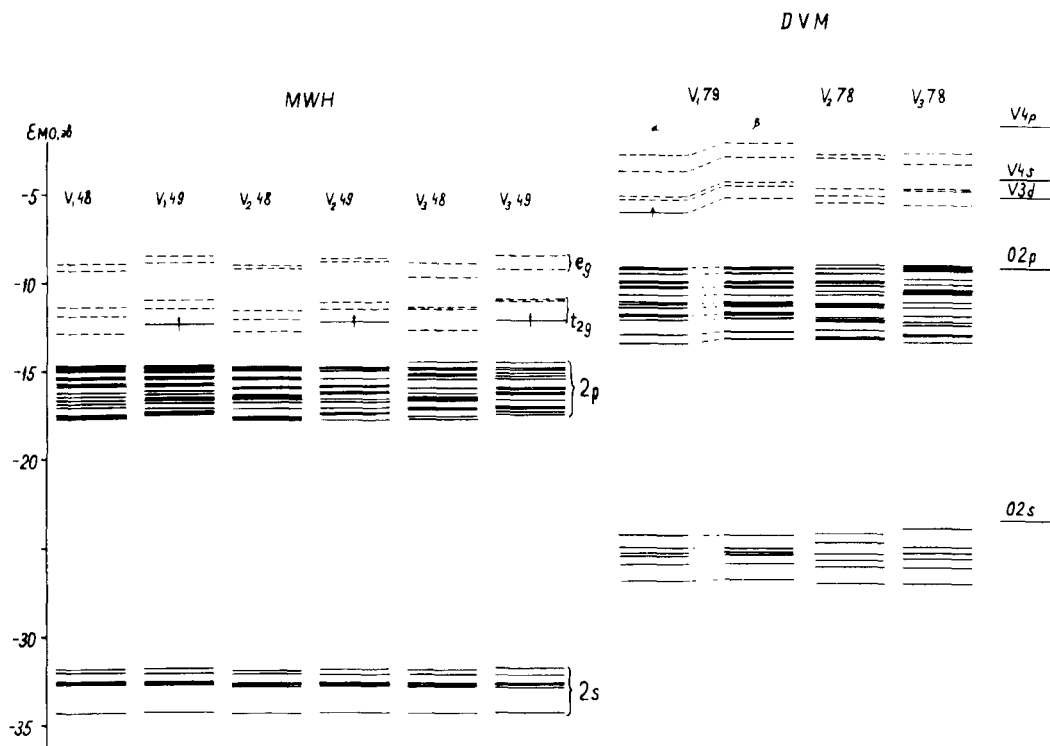


FIG. 5. MO energy diagram according to MWH and DVM calculations.

AO's in the DVM calculations are noticeably less than those in the MWH calculations. It also could be the result of non-self-consistency of the DVM calculations (22). The value of the effective charges on the vanadium according to the DVM calculations amounts to $\sim +2 e$ and has a tendency of decreasing when self-consistency on the charges is carried out. According to the results of the MWH calculations, the value of the effective charges amounts to about $+0.80$ – $0.84 e$ and indicates an essential role of covalency and inapplicability of the ionic model for the description of the electronic structure of $\text{NaV}_6\text{O}_{15}$.

It is interesting that, going from the V_n 48 cluster to the V_n 49 cluster, the effective charge on the vanadium changes only by $0.03 e$. The population of the $4s$ and $4p$ states decreases by $0.07 e$, and the population of the $3d$ states increases by $0.1 e$. So,

addition of an electron to the V_n 48 system causes the redistribution of the remaining electrons between the V atom and the oxygen environment, compensating the change of V effective charge. From Fig. 5, it is seen that an additional electron in the V_n 48 cluster leads to increase of the t_{2g} I -level energy by about $0.5 eV$. The energetics of other levels in this case practically do not change. The energies of the highest occupied t_{2g} I MO in $V_{1,49}$, $V_{2,49}$, and $V_{3,49}$ clusters are -12.58 , -12.39 , and $-12.30 eV$, respectively, i.e., the localization of an additional electron is profitable for the V_1 -type site. Thus, a possible model can be suggested, in which an electron localizes at one of the two clusters of the V_1 -type, and essentially does not change the population of the remaining cluster orbitals—one of the V_1 type, two of the V_2 type, and two of the V_3 type.

TABLE II

POPULATIONS OF ORBITALS AND BONDS, CONFIGURATIONS, AND CHARGES ON V ATOM FOR DIFFERENT SITES IN NaV₆O₁₅ ACCORDING TO DVM CALCULATIONS

Orbital	Populations of metal AO				
	α	β	$\alpha + \beta$	V ₂₇₈	V ₃₇₈
4s	0.0448	0.0391	0.0839	0.0783	0.0685
4p _x	0.0201	0.0181	0.0382	0.0457	0.0453
4p _y	0.0312	0.0291	0.0603	0.0276	0.0495
4p _z	0.0200	0.0178	0.0378	0.0411	0.0433
3d _{x²-y²}	0.2714	0.2320	0.5034	0.5192	0.5125
3d _{xz}	0.2862	0.2506	0.5368	0.4977	0.4901
3d _{z²}	0.2511	0.2139	0.4650	0.4607	0.5452
3d _{yz}	0.6794	0.1738	0.8532	0.3847	0.4568
3d _{xy}	0.5749	0.1889	0.7638	0.4480	0.3615
Electron configurations of V	4s ^{0.0448} 4p ^{0.0713} 3d ^{2.0630}	4s ^{0.0391} 4p ^{0.0650} 3d ^{1.0592}	4s ^{0.0839} 4p ^{0.1363} 3d ^{3.1222}	4s ^{0.0783} 4p ^{0.1144} 3d ^{2.3103}	4s ^{0.0685} 4p ^{0.1381} 3d ^{2.3661}
Charge on V	—	—	1.8778	2.5023	2.4273
Total bond population V-O	0.4241	0.4771	0.9012	0.9515	1.0420

It will be noted in such case that in the remaining five clusters an empty $t_{2g}I$ level proves to be situated lower in energy than the occupied $t_{2g}I$ level in the V₁₄₉ cluster. Therefore, if enough strong overlapping of the neighboring cluster wavefunction takes place, delocalization of the electron between the sites of different types, in which flattening of the energies of the lowest (partially occupied) $t_{2g}I$ orbitals for the clusters of all types is reached, can be energetically profitable. Assuming that the $t_{2g}I$ -level energy is linearly dependent on its population K , we tried to calculate fractional K_1 , K_2 , and K_3 numbers of the V₁, V₂, and V₃ sites so that the energy of the lowest (partially occupied) $t_{2g}I$ orbital was equal for all the sites. It appeared to be impossible to satisfy all these requirements, since, in the V₃₄₈ cluster, the lowest 3d-level energy is of too great a value. Excluding from consideration V₃-type sites,

fractional populations of V₁ and V₂ sites have been calculated. Satisfying the condition of flattening of the lowest partially occupied 3d-level energies and taking into account the condition $2(K_1 + K_2) = 1$, we obtained $K_1 = 0.465$ and $K_2 = 0.035e$. The calculations performed of V_{148.465} and V_{248.035} clusters indeed showed that the energies of the partially occupied $t_{2g}I$ levels practically have the same energies (-12.89 and -12.86 eV) and these values are less than the energy of the lowest unoccupied $t_{2g}I$ level of the V₃₄₈ (-12.80 eV) cluster.

It should be noted that in the model proposed the fractional populations for clusters were obtained neglecting the interactions between clusters. Taking into account such interaction, some population flattening on the sites can be expected to take place and the degree of delocalization to increase. When the Na valence electron concentration

increases, such a model will result in an increase of the degree of delocalization. For instance, appropriate fractional populations for two electrons per formula unit are $n_1 = 0.6$, $n_2 = 0.3$, and $n_3 = 0.1$. This shows that when the Na content increases in $\text{Na}_x\text{V}_6\text{O}_{15}$, delocalization must grow. Indeed, the measurements of electrical conductivity and magnetic susceptibility of $\text{Cu}_x\text{V}_6\text{O}_{15}$ (9) showed that the properties of this compound assume more and more metallic character as x rises.

The Calculation of X-Ray Emission Spectra Intensity

The intensities of the X-ray emission $K_{\beta''\beta_5}$ and L_α spectra of V in $\text{NaV}_6\text{O}_{15}$ have been found using MWH calculations of the V_1 , V_2 , and V_3 clusters with 48,49 valence electrons and fractional populations for the V_1 and V_2 sites. The intensities were evaluated by the formula $I_i \sim n_i \sum_j C_{ij}^2$ (23), where C_{ij} are the coefficients of the j th atomic function ($j = 4p$ for $K_{\beta''\beta_5}$ spectra and $j = 3d, 4s$ for L_α spectra) of the i th MO and n_i is the population of the i level. Linear $VK_{\beta''\beta_5}$ and VL_α spectra were built up for all the clusters calculated. Plotting of the summary spectra, appropriate to the two variants of Na valence electron localization under discussion, was then carried out. In the first case, spectra appropriate to V_{149} , V_{248} , $2V_{248}$, $2V_{348}$ were summarized: $I = \frac{1}{2}(I_{V_{149}} - I_{V_{148}}) - I_{V_{248}} - I_{V_{348}}$. In the second case, $V_{148.468}$, $V_{248.035}$, and V_{348} spectra were superimposed. The linear spectra were then smeared out, taking into account the Lorentz form of the line. The width was $\Delta E = 1.5$ eV and fitted to best coincidence with the experimental spectra. The spectra corresponding to the two models of localization practically do not differ.

In Fig. 6, $VK_{\beta''\beta_5}$ and VL_α spectra calculated for the model of fractional population of V_1 and V_2 sites are compared with experimental spectra of vanadium in $\text{NaV}_6\text{O}_{15}$ (1).

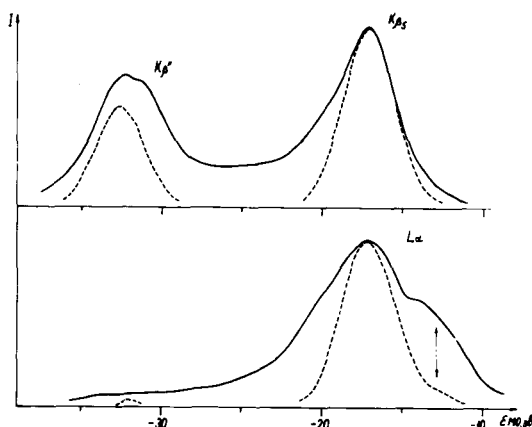


FIG. 6. Comparison of experimental (solid line) and calculated (broken line) $K_{\beta''\beta_5}$ and L_α spectra of V for $\text{NaV}_6\text{O}_{15}$ polycrystals.

As is seen, the calculations correlate well with the experimental spectra. They describe the energy separation of the $K_{\beta''}$ and K_{β_5} subbands and their intensities. These subbands are due to electron transitions from $O2p$ and $O2s$ bands to the V_{1s} level owing to $V4p-O2p$, $O2s$ hybridization. The main peak of the VL_α spectrum is connected with X-ray transitions of electrons from the $O2p$ band to the $V2p$ level due to $V3d-Osp$ hybridization. The less intense short-wave subband of the VL_α spectrum is due to transition from the lowest level of the $V3d$ band, in which the $V_{148.465}$ cluster gives the main contribution. The position of such a level is marked in Fig. 6 by the arrow. The energy separation of the subband for the calculated VL_α spectrum agrees well with the experimental value. In the VL_α spectrum, the position of the $O2s$ band is also reflected, due to $V3d-O2s$ hybridization. However, the intensity of the short-wave subband of the VL_α spectrum is underestimated in our calculation. It should be noted that in the calculated VL_α spectrum for V_2O_5 this subband is absent (24) although the experiment shows a considerable intensity (25, 26). The energy position of such a subband coincides

with vacant orbitals of (VO₆)⁷⁻ clusters in V₂O₅ and the origin of the short-wave subband can be connected with electron transitions from excited states, populated during the process of generation of X-ray radiation. An analogous mechanism can be realized also in the case of VL_α spectra for the bronzes, and it can result in an increase of the short-wave subband intensity experimentally.

The intensity calculation of VK_{β''β₅} spectra polarized along the **b** axis and within the plane perpendicular to this axis has been carried out using the relations:

$$I_{\parallel,i} \sim n_i C_{i,4py}^2; \quad I_{\perp,i} \sim \frac{1}{2} n_i (C_{i,4px}^2 + C_{i,4pz}^2).$$

Figure 7 shows calculated polarized spectra for a model with fractional populations of

the V₁ and V₂ sites together with the experimental spectra. It is seen that good coincidence of subband positions and the structure of the K_{β''} subband exists for all three sites. Indeed, the three-bond character of the K_{β''} subband, established by experiment, is revealed only in the I_⊥ spectrum. In the theoretical I_∥ spectrum, the contribution to the K_{β''} subband gives only one orbital. A possible source of the low-energy structure (3) in the experimental ε_∥**b** spectrum was discussed above. The results obtained confirm the proposed interpretation of the K_{β''} subband structure as being connected with the existence of different bond lengths in the nearest environment of the V atom, i.e., with nonequivalent positions of the oxygen atoms. However, the main effects of

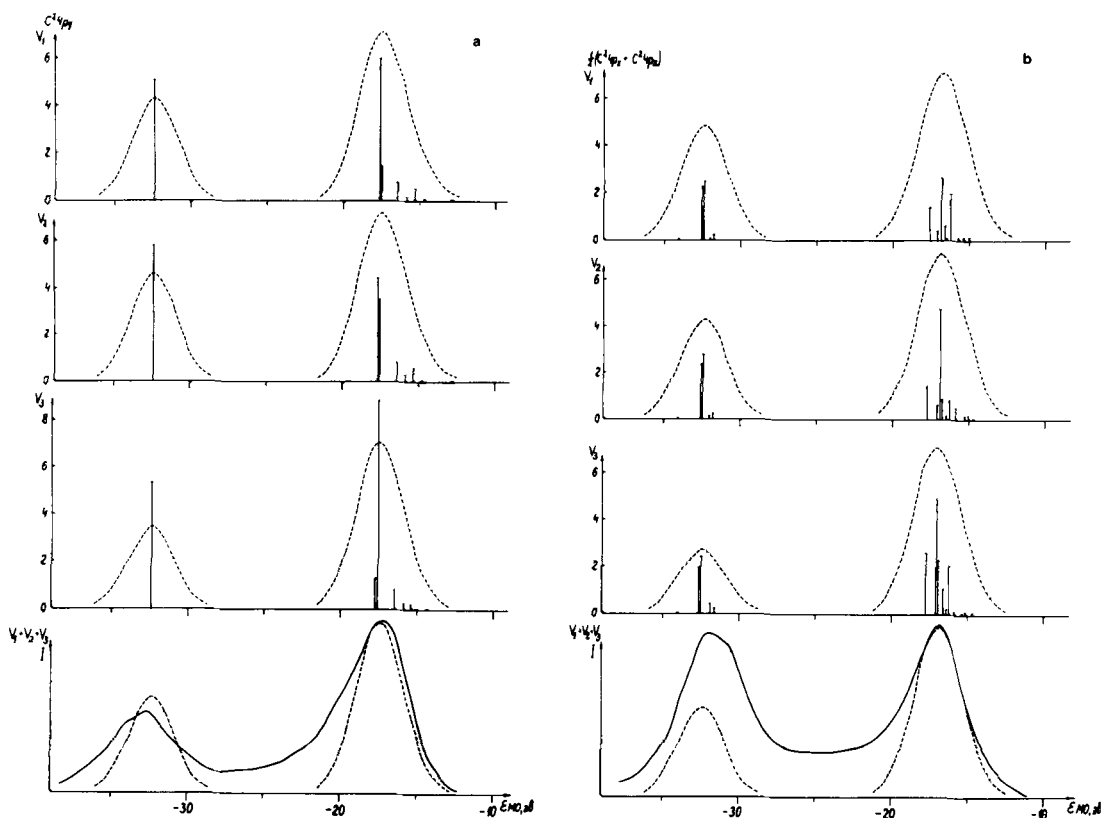


FIG. 7. Calculated polarized K_{β''β₅} spectra of V for NaV₆O₁₅ monocystals (for different sites) and comparison of summary anisotropy spectra with experimental spectra (solid line): (a) ε_∥**b**; (b) ε_⊥**b**.

the anisotropy (which occur in the redistribution of the $K_{\beta'\beta_5}$ subband intensity) are not explained by the calculation.

On the one hand, the theoretical calculated $K_{\beta'\beta_5}$ spectrum for a cluster with a central V atom of the V_1 type shows the presence of some anisotropy, qualitatively similar to that in the experiment. However, the calculations performed for clusters with V_3 -type central atoms give anisotropy of opposite character and, as a result, the summary theoretical spectra composed of V_1 , V_2 , and V_3 site contributions do not coincide with experimental spectra (Fig. 7). Calculations of anisotropic spectra for a model in which an electron is localized on the V_1 site lead to the same result.

Inadequacy of the polarized spectra intensity description could be connected with neglect of the second coordination sphere of the V atom.

Discussion of Properties

Let us consider the connection of the results obtained with well-known physical properties of oxygen-vanadium $\text{NaV}_6\text{O}_{15}$ bronze. The quantum-chemical calculations show that valence electron delocalization between V_1 and V_2 sites is more energetically favorable. It correlated with experimental data showing electron delocalization in an oxygen-vanadium sublattice (1, 9, 10). A partly occupied $t_{2g}1$ orbital represents mainly an admixture of $V3d_{yz}$ and $V3d_{xy}AO$ on V_1 and V_2 sites. Furthermore, this MO has on the V_1 site considerable admixture of ligand wavefunctions in the following decreasing order of contribution: $2p_{xz}AO$ of the O_2 atom, $2p_yAO$ of O_5 and O_3 atoms. The main contributions of the ligand wavefunctions on the V_2 site are characterized by the set: $2p_{xz}AO$ of O_3 atom and $2p_yAO$ of O_1 and O_5 atoms. So, delocalization of the valence electron along the b axis in V_1 and V_2 site chains through the intermediate oxygen O_2 and O_3 atoms is most probable. Charge

transfer in the ac plane through intermediate oxygen O_5 and O_1 atoms is limited by the V_3 sites, which have in our model a zero population of conduction electrons. However, even if the V_3 sites are supposed to have a limited population, charge transfer in the ac plane will be difficult. It follows from the form of the $t_{2g}1$ MO wavefunction on this site, which is described mainly by $V3d_{xy}$ states, $2p_yAO$ of O_5 atoms, and $2p_xAO$ of O_7 atom, that delocalization in the b -axis direction is less than that in the V_1 and V_2 site chains. So, it follows from the calculations that electrical conductivity of $\text{NaV}_6\text{O}_{15}$ should have a pronounced quasi-one-dimensional character. Delocalization of the electrons is not due to direct metal-metal interaction because the smallest V-V distance in this bronze amounts to 3.12 Å (V_1 - V_2) whereas the critical metal-metal distance required for bond formation is considerably less (2.94 Å (27)). As has been mentioned, these compounds are semiconductors of the polaron type (7, 8), characterized by electron hopping between localized states. For simultaneously satisfying the requirements of localization and delocalization, it is necessary to suppose formation of domains composed of several V atoms in which the electrons are delocalized (1, 9). Electrical conductivity in such case would be effected by thermally activated hopping of electrons between domains. The cause of such domain formation is not clear, but it may be induced by disordered arrangement of alkali atoms or Peierls instability. The data on EPR spectra temperature dependence for these bronzes, which show an anomaly of the spin-lattice interaction at about 350°C (28), are in favor of the latter supposition. At this temperature, after vacuum annealing, $\text{NaV}_6\text{O}_{15}$ bronzes reveal a one-dimensional semiconductor-metal phase transition (4, 5). One can suppose that, in unannealed bronze, the additional oxygen atoms which stabilize the lattice distortion and are removed in process of annealing oppose this phase transition

(4, 5). However, the anomaly of the spin-lattice interaction remains and leads to the one-dimensional semiconductor-metal transition. Such an anomaly can be connected with softening of phonons having a $2k_F$ wave vector. In this connection, it would be of interest to investigate the phonon spectrum (by inelastic neutron scattering) and look for presence of a $2k_F$ period sublattice (by diffuse scattering of X rays) for further understanding of the physical nature of MV_6O_{15} bronzes.

References

1. V. M. CHERKASHENKO, E. Z. KURMAEV, V. E. DOLGIKH, A. A. FOTIEV, AND V. L. VOLKOV, VINITI, N. 2408-75 Dep.
2. A. D. WADSLEY, *Acta Crystallogr.* **8**, 596 (1955).
3. R. P. OZEROV, *Kristallografia* **2**, 22 (1957).
4. V. K. KAPUSTKIN, Avotreferat kand. dissert., Sverdlovsk (1975).
5. V. K. KAPUSTKIN, V. L. VOLKOV, AND A. A. FOTIEV, *J. Solid State Chem.* **19**, 359 (1976).
6. J. GENDELL, R. M. COTTS, AND M. J. SIENKO, *J. Chem. Phys.* **37** 220 (1962).
7. J. B. GOODENOUGH, *J. Solid State Chem.* **1**, 349 (1970).
8. J. H. PERLSTEIN AND M. J. SIENKO, *J. Chem. Phys.* **48**, 174 (1968).
9. A. CASALOT AND P. HAGENMULLER, *J. Phys. Chem. Solids* **30**, 1341 (1969).
10. D. KAPLAN AND A. ZYLBERSTEIN, *J. Phys. Lett. (Paris)* **37**, L-123 (1976).
11. V. I. MATISKIN, Avtoreferat kand, dissert., Kiev (1971).
12. G. DREGER AND O. BRUMMER, *Izv. Akad. Nauk SSSR ser. Fiz.* **40**, 2437 (1976).
13. CHR. BEYRENTHER, R. HIREL, AND G. WIECH, *Ber. Bunsenes. Phys. Chem.* **79**, 1081 (1975).
14. C. J. BALLHAUSEN AND H. B. GRAY, "Molecular Orbital Theory", Benjamin, New York (1964).
15. H. BACH, A. VISTE, AND H. B. GRAY, *Theor. Chim. Acta* **3**, 458 (1965).
16. H. BACH, A. VISTE, AND H. B. GRAY, *J. Chem. Phys.* **44**, 10 (1966).
17. V. A. GUBANOV, B. G. KASIMOV, AND E. Z. KURMAEV, *J. Phys. Chem. Solids* **36**, 861 (1975).
18. N. I. LAZUKOVA, V. A. GUBANOV, AND R. N. PLETNEV, *Int. J. Quant. Chem.* **9**, 691 (1975).
19. D. E. ELLIS AND G. S. PAINTER, *Phys. Rev.* **32**, 2887 (1970).
20. F. W. AVERILL AND D. E. ELLIS, *Chem. Phys.* **59**, 6412 (1973).
21. F. HERMAN AND S. SKILLMAN, "Atomic Structure Calculations," Prentice-Hall, Englewood Cliffs, N.J. (1963).
22. V. A. GUBANOV AND D. E. ELLIS, *Zh. Strukt. Khim.* **17**, 962 (1976).
23. V. I. NEFEDOV, "Stroenie molekul i khimicheskaya svyaz" Vol. 3, VINITI, Moskva (1975).
24. V. A. GUBANOV, N. I. LAZUKOVA AND E. Z. KURMAEV, *Izv. Sib. Otd. Akad. Nauk SSSR Ser. Khim.* **4**, No. 9, 18(1975).
25. D. W. FISHER, *J. Appl. Phys.* **41**, 3561 (1970).
26. V. M. CHERKASHENKO, V. E. DOLGIKH, E. Z. KURMAEV, AND A. A. FOTIEV, *J. Solid State Chem.* **22**, 217 (1977).
27. J. B. GOODENOUGH, *Czech. J. Phys. B* **17**, 304 (1967).
28. R. N. PLETNEV, V. K. KAPUSTKIN, V. L. VOLKOV, AND A. A. FOTIEV, *Vestn. Khim. O. im. D.I. Mendeleeva* **19**, 100 (1974).